

Hydrothermal phase equilibria in $\text{Er}_2\text{O}_3\text{-H}_2\text{O-CO}_2$ and $\text{Tm}_2\text{O}_3\text{-H}_2\text{O-CO}_2$ systems

IFTIQHAR MOHAMED, J A K TAREEN and T R N KUTTY*

Mineralogical Institute, University of Mysore, Manasa Gangotri, Mysore 570 006, India
* Department of Inorganic and Physical Chemistry, Indian Institute of Science, Bangalore 560 012, India

MS received 6 October 1983

Abstract. Isobaric phase equilibria in $\text{Er}_2\text{O}_3\text{-H}_2\text{O-CO}_2$ and $\text{Tm}_2\text{O}_3\text{-H}_2\text{O-CO}_2$ systems have been determined at 650 and 1300 bars and temperature range of 100–800°C. The equilibria depend on the mole fraction of CO_2 in the coexisting fluid. The stable phases: $\text{Ln}(\text{OH})_3$, $\text{Ln}_2(\text{CO}_3)_3 \cdot 3\text{H}_2\text{O}$, $\text{Ln}(\text{OH})\text{CO}_3$ —orthorhombic, $\text{Ln}_2\text{O}_2\text{CO}_3$ —hexagonal, LnOOH and Ln_2O_3 —cubic are common to both the systems. Additional phases observed in the thulium system are $\text{Tm}_2\text{O}(\text{OH})_2\text{CO}_3$ and $\text{Tm}_6(\text{OH})_4(\text{CO}_3)_7$. Two other phases isolated are $\text{Tm}_6\text{O}_2(\text{OH})_8(\text{CO}_3)_3$ and $\text{Tm}_4(\text{OH})_6(\text{CO}_3)_3$ which are stabilised only in the presence of alkali impurities. Stability field of $\text{Ln}(\text{OH})_3$ is limited to $X_{\text{CO}_2} < 0.01$. $\text{Tm}(\text{OH})\text{CO}_3$ does not stabilise at low X_{CO_2} ; therefore TmOOH coexists with all the phases other than $\text{Tm}_6(\text{OH})_4(\text{CO}_3)_7$. When $X_{\text{CO}_2} = 1$, the stable phases are $\text{Tm}_2\text{O}_2\text{CO}_3$ and Tm_2O_3 in the order of increasing temperature. The normal carbonate, $\text{Tm}_2(\text{CO}_3)_3 \cdot 8\text{H}_2\text{O}$ has no stability at higher pressures.

Keywords. Hydrothermal equilibria; lanthanide carbonates; basic carbonates; thulium.

1. Introduction

Ternary heterogeneous systems: $\text{Ln}_2\text{O}_3\text{-H}_2\text{O-CO}_2$ ($\text{Ln} = \text{Lanthanides}$), under hydrothermal conditions are important for mineral syntheses and crystal growth of carbonates, hydroxides and oxides of lanthanides. Solid phases isolated from high pressure experiments (Christensen 1970; Chai and Mroczkowski 1978) as well as experiments at low temperature and one atmosphere pressure (Dexpert *et al* 1972; Sawyer *et al* 1973; Caro and Lemaitre-Blaise 1970) were isostructural with minerals like lanthanite, tenerite (Tareen *et al* 1980a) bastnaesite and ancylite. The present authors have investigated systematically the phase diagrams in different $\text{Ln}_2\text{O}_3\text{-H}_2\text{O-CO}_2$ systems. Phase diagrams for the lanthanides of the ceric group have been reported earlier (Kutty *et al* 1978; Tareen and Kutty 1980). Extending this work to heavier lanthanides, we have found that there are new phases stabilised under pressure. Marked differences are observed in $\text{Tm}_2\text{O}_3\text{-H}_2\text{O-CO}_2$ system, when compared to the corresponding Er_2O_3 system.

2. Experimental

Er_2O_3 (Leico Industries, New York) and Tm_2O_3 (Koch-light Labs, U.K) were of 99.99% purity. Details of experiments for hydrothermal equilibria studies and

* To whom all correspondence should be addressed.

maintenance of known partial pressures of CO_2 and H_2O are as reported earlier (Kutty *et al* 1978; Viswanathiah *et al* 1978). Methods of chemical analyses were reported by Tareen and Kutty (1980). X-ray powder patterns were taken with Philips PW 1041 diffractometer. IR spectra were recorded on Perkin Elmer 597 spectrometer or Carl-Zeiss Jena UR 10 in the range of $400\text{--}4000\text{ cm}^{-1}$ both in KBr and Nujol mull.

3. Results and discussion

Isobaric (650 bars) phase diagram of $\text{Er}_2\text{O}_3\text{--H}_2\text{O--CO}_2$ (figure 1) showed six stable phases: $\text{Er}(\text{OH})_3$, $\text{Er}_2(\text{CO}_3)_3 \cdot 3\text{H}_2\text{O}$, $\text{Er}(\text{OH})\text{CO}_3$ —orthorhombic, $\text{Er}_2\text{O}_2\text{CO}_3$ —hexagonal, ErOOH —monoclinic and Er_2O_3 —cubic. Isobaric phase diagrams at 1300 bars exhibited the same set of stable phases, except that the area of hydroxides— $\text{Er}(\text{OH})_3$ and ErOOH —shift to slightly lower X_{CO_2} (mole fraction of CO_2) values. There are six triple-points; which are invariant points at constant P-T values; temperature-wise the lowest one is around 130°C involving $\text{Er}(\text{OH})_3$, $\text{Er}_2(\text{CO}_3)_3 \cdot 3\text{H}_2\text{O}$ and $\text{Er}(\text{OH})\text{CO}_3$; the highest temperature triple-point is that of $\text{ErOOH--Er}_2\text{O}_2\text{CO}_3\text{--Er}_2\text{O}_3$. Compared to the phase diagram of $\text{Gd}_2\text{O}_3\text{--H}_2\text{O--CO}_2$ (Tareen and Kutty 1980), the field of trihydroxide is broader, extending up to $X_{\text{CO}_2} = 0.05$. For the lighter lanthanides, stability of $\text{Ln}(\text{OH})_3$ is very limited ($X_{\text{CO}_2} = 0.008$ for Nd; $X_{\text{CO}_2} = 0.003$ for Gd). Around 260°C , $\text{Er}(\text{OH})_3$ converts to ErOOH and further to Er_2O_3 —cubic at 655°C , when X_{CO_2} approaches zero. At higher values, $\text{Er}(\text{OH})_3$ transforms to $\text{Er}_2(\text{CO}_3)_3 \cdot 3\text{H}_2\text{O}$ which is isostructural with the mineral tengerite. The crystalline phase equivalent to lanthanite, $\text{Ln}_2(\text{CO}_3)_3 \cdot 8\text{H}_2\text{O}$, is not stabilised under hydrothermal conditions. With

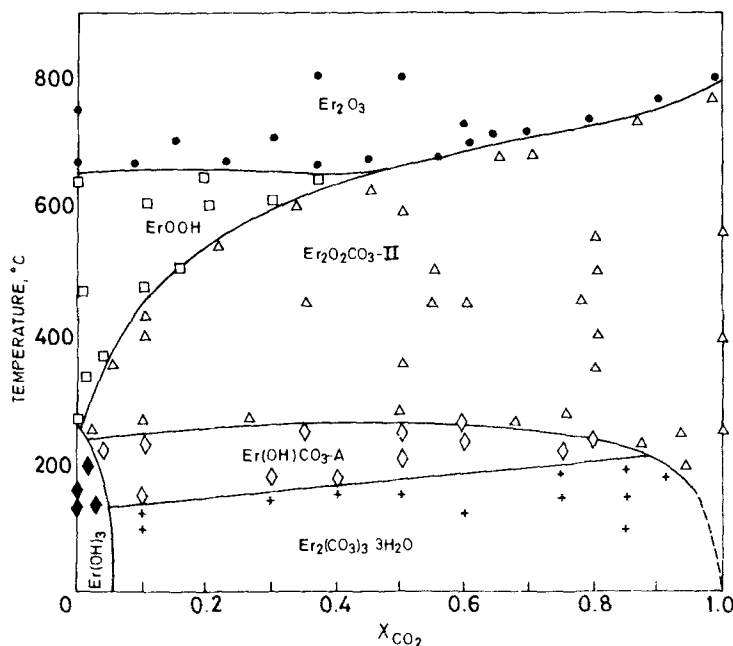


Figure 1. $T\text{--}X_{\text{CO}_2}$ phase diagram for $\text{Er}_2\text{O}_3\text{--H}_2\text{O--CO}_2$ system at 650 bars.

rise in temperature, $\text{Er}_2(\text{CO}_3)_3 \cdot 3\text{H}_2\text{O}$ directly converts to $\text{Er}(\text{OH})\text{CO}_3$ with orthorhombic symmetry (isostructural with the mineral ancylite). There is no hydrothermal stability for $\text{Er}(\text{OH})\text{CO}_3$ —hexagonal, which is the prevalent phase in lanthanides lighter than Gd. In $\text{Nd}_2\text{O}_3\text{--H}_2\text{O--CO}_2$ system, the stable $\text{Nd}(\text{OH})\text{CO}_3$ phase, is equivalent to bastnaesite while for Gd, both hexagonal and orthorhombic phases of $\text{Gd}(\text{OH})\text{CO}_3$ are stable. There is X_{CO_2} -dependent phase transformation at 1500 bars, in $\text{Gd}(\text{OH})\text{CO}_3$. In figure 1, $\text{Er}_2\text{O}_2\text{CO}_3$ —hexagonal, with a broader field of stability, is stable at higher temperatures. With increasing X_{CO_2} , it transforms to Er_2O_3 .

Figures 2A–C gives the isothermal sections of the three-component system at 650 bars, showing the compositional stability of the various phases at 150°, 550° and 700°C respectively. The section at 150°C (figure 2A) shows that $\text{Er}(\text{OH})_3$, $\text{Er}(\text{OH})\text{CO}_3$ and $\text{Er}_2(\text{CO}_3)_3 \cdot 3\text{H}_2\text{O}$ become stable, as X_{CO_2} value increases. $\text{Er}_2\text{O}_2\text{CO}_3$ phase is stable at $X_{\text{CO}_2} = 1$ i.e. in the system nearly free of H_2O . The section at 550°C (figure 2B) has only two stable phases, ErOOH and $\text{Er}_2\text{O}_2\text{CO}_3$ in the increasing order of X_{CO_2} . The section at 700°C shows that Er_2O_3 and $\text{Er}_2\text{O}_2\text{CO}_3$ are the only persistent phases in equilibrium with the H_2O -free fluid.

Based on 72 experimental equilibrium points, $T\text{--}X_{\text{CO}_2}$ diagram for $\text{Tm}_2\text{O}_3\text{--H}_2\text{O--CO}_2$ system has been constructed (figure 3). This diagram is different from those of the previously reported $\text{Ln}_2\text{O}_3\text{--H}_2\text{O--CO}_2$ system including that of Er_2O_3 . $\text{Tm}(\text{OH})\text{CO}_3$ disappears at higher X_{CO_2} , and at higher temperature, giving way

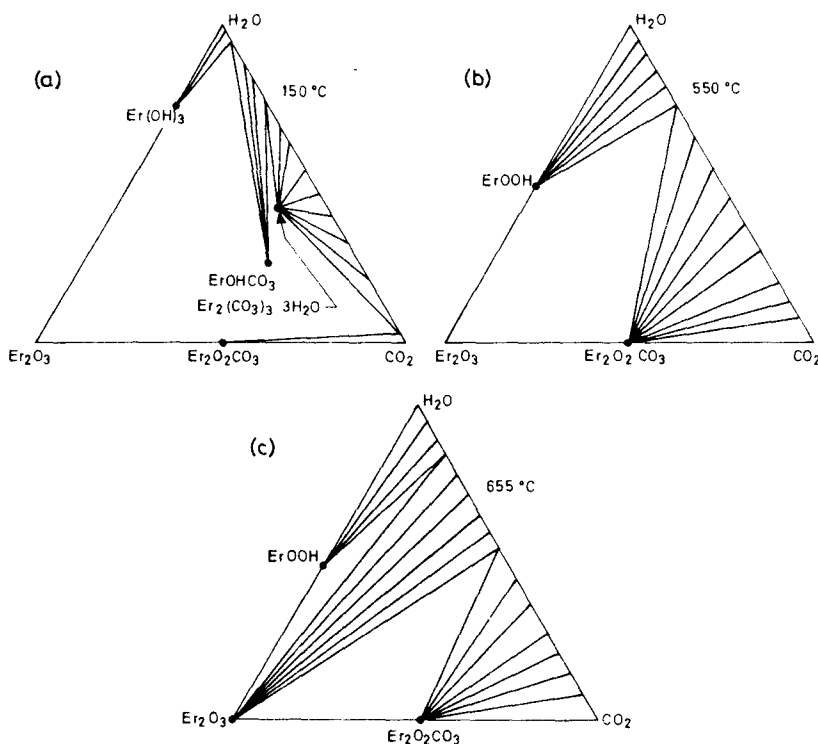


Figure 2. Isothermal sections at a. 150°C. b. 550°C and c. 700°C for $\text{Er}_2\text{O}_3\text{--H}_2\text{O--CO}_2$ at 650 bars.

to hitherto unreported hydroxy carbonates. Besides, $\text{Tm}(\text{OH})\text{CO}_3$ is not stable at very low concentration of CO_2 ($X_{\text{CO}_2} \sim 0.01$) and converts to TmOOH . The new carbonate phases with definite reproducibility are $\text{Tm}_6(\text{OH})_4(\text{CO}_3)_7$, and $\text{TmO}(\text{OH})_2\text{CO}_3$. The phase boundaries between $\text{Tm}_6(\text{OH})_4(\text{CO}_3)_7$, $\text{Tm}(\text{OH})\text{CO}_3$ and $\text{Tm}_2\text{O}(\text{OH})_2\text{CO}_3$ are very sensitive to small variations in X_{CO_2} values and minor temperature fluctuations. The reason will be evident when the isothermal sections are considered. The boundaries are tentatively demarcated with dashed lines (figure 3) though the diagram is constructed from data points of highest reproducibility. Within the boundary of $\text{Tm}_2\text{O}(\text{OH})_2\text{CO}_3$ and $\text{Tm}(\text{OH})\text{CO}_3$, two more phases could be isolated $\text{Tm}_6\text{O}_2(\text{OH})_8(\text{CO}_3)_3$ and $\text{Tm}_4(\text{OH})_6(\text{CO}_3)_3$. These phases could only sparingly be reproduced and depend on alkali contamination in ppm concentrations. Since these phases may not be stable in highly pure $\text{Tm}_2\text{O}_3\text{-H}_2\text{O-CO}_2$ system, they are not plotted in figure 3. The other stable phases *viz* $\text{Tm}(\text{OH})_3$, TmOOH , $\text{Tm}_2\text{O}_2\text{CO}_3$ —hexagonal and Tm_2O_3 —cubic are identical to those of Er_2O_3 system. The complexity in the nature of stable carbonates is only in the region between $\text{Tm}_2(\text{CO}_3)_3 \cdot 3\text{H}_2\text{O}$ and $\text{Tm}_2\text{O}_2\text{CO}_3$. Another new feature in figure 3 is the coexistence of TmOOH with $\text{Tm}_2(\text{CO}_3)_3 \cdot 3\text{H}_2\text{O}$, $\text{Tm}(\text{OH})\text{CO}_3$, $\text{Tm}_2\text{O}(\text{OH})_2\text{CO}_3$ and $\text{Tm}_2\text{O}_2\text{CO}_3$ whereas in Er_2O_3 system, ErOOH converts only to $\text{Er}_2\text{O}_2\text{CO}_3$ with increased X_{CO_2} .

Figures 4A–C show the isothermal sections of $\text{Tm}_2\text{O}_3\text{-H}_2\text{O-CO}_2$ at 650 bars. At 150°C , $\text{Tm}(\text{OH})_3$, $\text{Tm}_2(\text{CO}_3)_3 \cdot 3\text{H}_2\text{O}$, $\text{Tm}(\text{OH})\text{CO}_3$, and $\text{Tm}_6(\text{OH})_4(\text{CO}_3)_7$ are the stable phases. At this temperature, $\text{Tm}_2\text{O}_2\text{CO}_3$ is barely stable in the H_2O -free system. At 350°C , these phases are replaced by TmOOH , $\text{Tm}_2\text{O}(\text{OH})_2\text{CO}_3$ and $\text{Tm}_2\text{O}_2\text{CO}_3$ (figure 4B). At 625°C , $\text{Tm}_2\text{O}_2\text{CO}_3$ and Tm_2O_3 are the only stable phases (figure 4C). It is evident from figure 4A, B that the isothermal stability fields of $\text{Tm}(\text{OH})\text{CO}_3$, $\text{Tm}_2\text{O}(\text{OH})_2\text{CO}_3$ and $\text{Tm}_2(\text{CO}_3)_3 \cdot 3\text{H}_2\text{O}$ are very narrow such that slight

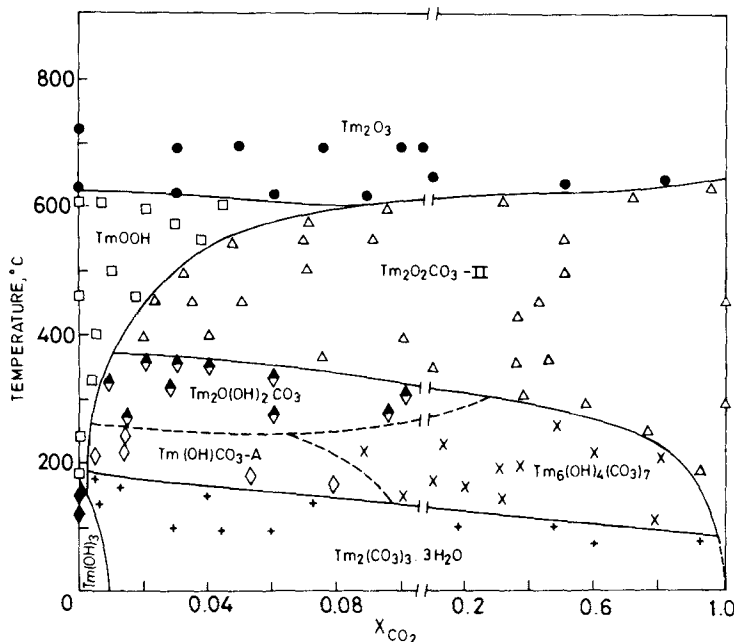


Figure 3. $T\text{-}X_{\text{CO}_2}$ phase diagram for $\text{Tm}_2\text{O}_3\text{-H}_2\text{O-CO}_2$ system at 650 bars.

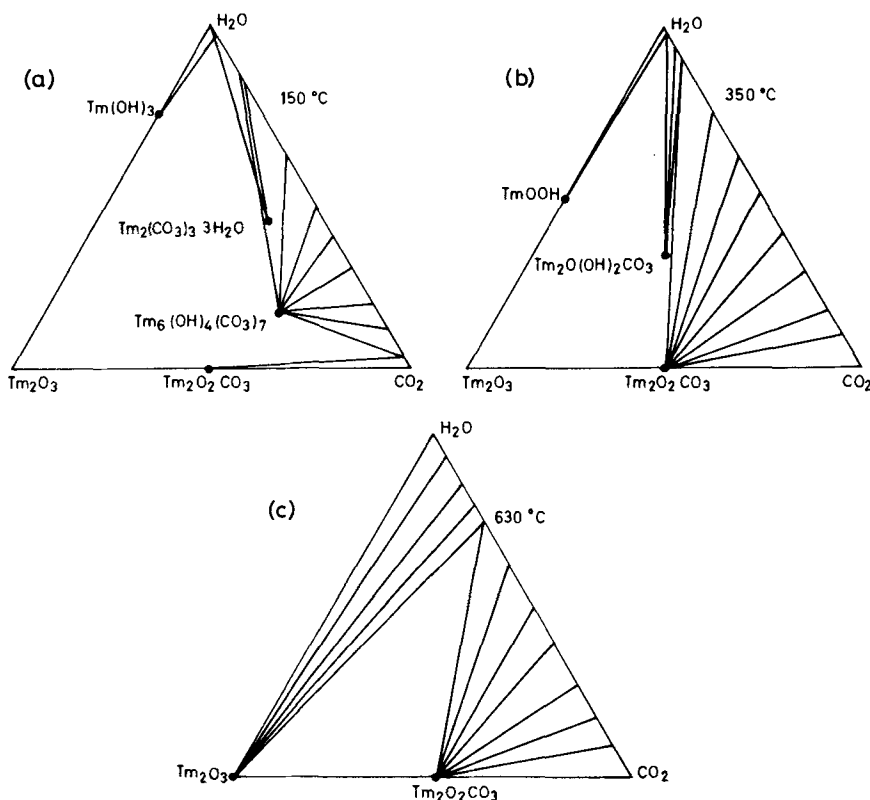


Figure 4. Isothermal sections at a. 150°C, b. 350°C and c. 630°C for $\text{Tm}_2\text{O}_3\text{-H}_2\text{O-CO}_2$ at 650 bars.

compositional difference in the starting materials will alter the coexisting solid phases. The tie-lines between $\text{Tm}_2(\text{CO}_3)_3 \cdot 3\text{H}_2\text{O}$, $\text{Tm}(\text{OH})\text{CO}_3$, $\text{Tm}_2\text{O}(\text{OH})_2\text{CO}_3$ and $\text{Tm}_6(\text{OH})_4(\text{CO}_3)_7$ overlap considerably. Hence the demarcation of boundaries between these phases in figure 3 is difficult.

Following are the chemical equilibria involved in $\text{Tm}_2\text{O}_3\text{-H}_2\text{O-CO}_2$ system:

- (i) $2 \text{Tm}(\text{OH})_3 + 3\text{CO}_2 = \text{Tm}_2(\text{CO}_3)_3 \cdot 3\text{H}_2\text{O}$
- (ii) $\text{Tm}_2(\text{CO}_3)_3 \cdot 3\text{H}_2\text{O} = 2 \text{Tm}(\text{OH})\text{CO}_3 + 2\text{H}_2\text{O} + \text{CO}_2$,
- (iii) $2 \text{Tm}(\text{OH})\text{CO}_3 = \text{Tm}_2\text{O}(\text{OH})_2\text{CO}_3 + \text{CO}_2$,
- (iv) $\text{Tm}_2(\text{CO}_3)_3 \cdot 3\text{H}_2\text{O} = \text{Tm}_2\text{O}(\text{OH})_2\text{CO}_3 + 2\text{CO}_2 + 2\text{H}_2\text{O}$,
- (v) $3 \text{Tm}_2\text{O}(\text{OH})_2\text{CO}_3 + 4 \text{CO}_2 + 0.5 \text{H}_2\text{O} = \text{Tm}_6(\text{OH})_4(\text{CO}_3)_7$,
- (vi) $\text{Tm}(\text{OH})_3 = \text{TmOOH} + \text{H}_2\text{O}$,
- (vii) $\text{TmOOH} + \text{CO}_2 = \text{Tm}(\text{OH})\text{CO}_3$,
- (viii) $2 \text{TmOOH} + \text{CO}_2 = \text{Tm}_2\text{O}(\text{OH})_2\text{CO}_3$,
- (ix) $\text{Tm}_2\text{O}(\text{OH})_2\text{CO}_3 = \text{Tm}_2\text{O}_2\text{CO}_3 + \text{H}_2\text{O}$,
- (x) $2 \text{TmOOH} + \text{CO}_2 = \text{Tm}_2\text{O}_2\text{CO}_3 + \text{H}_2\text{O}$,
- (xi) $\text{Tm}_6(\text{OH})_4(\text{CO}_3)_7 = 3 \text{Tm}_2\text{O}_2\text{CO}_3 + 4\text{CO}_2 + 2\text{H}_2\text{O}$,
- (xii) $2 \text{TmOOH} = \text{Tm}_2\text{O}_3 + \text{H}_2\text{O}$,
- (xiii) $\text{Tm}_2\text{O}_2\text{CO}_3 = \text{Tm}_2\text{O}_3 + \text{CO}_2$.

3.1 Characterisation of carbonate phases

Table 1 gives the chemical composition of stable phases isolated from hydrothermal experiments. The agreement between Ln_2O_3 , H_2O and CO_2 contents observed and calculated according to the formula given in the last column is reasonable in all the cases. The phase purity of analysed samples is confirmed by both x-ray powder pattern and IR absorption spectrum.

The unit cell constants derived from x-ray powder diffraction data for the phases identical to those from Gd_2O_3 system are listed in table 2. The indexed powder data for $\text{Ln}_2(\text{CO}_3)_3 \cdot 3\text{H}_2\text{O}$, $\text{Ln}(\text{OH})_3$, LnOOH , $\text{Ln}_2\text{O}_2\text{CO}_3$ (hexagonal), $\text{Ln}(\text{OH})\text{CO}_3$ (orthorhombic) and Ln_2O_3 (cubic) are reported earlier for many of the lanthanides (Sawyer *et al* 1973; Tareen *et al* 1980a,b; Kutty *et al* 1978; Tareen and Kutty 1980; Chai and Mroczkowski 1978). The indexed x-ray data for $\text{Tm}_2\text{O}(\text{OH})_2\text{CO}_3$ and $\text{Tm}_6(\text{OH})_4(\text{CO}_3)_7$ are given in table 3 Christensen (1973) and Chai and Mroczkowski (1978) have reported $\text{Y}_2\text{O}(\text{OH})_2\text{CO}_3$ as a stable phase under hydrothermal conditions. The x-ray data for the metastable phases $\text{Tm}_6\text{O}_2(\text{OH})_8(\text{CO}_3)_3$ and $\text{Tm}_4(\text{OH})_6(\text{CO}_3)_3$

Table 1. Chemical analysis of hydrothermally stable phases.

Lanthanide	Ln_2O_3		H_2O		CO_2		Chemical formula
	obsd	calc	obsd	calc	obsd	calc	
Ln = Er	87.7	87.63	12.43	12.37	—	—	$\text{Er}(\text{OH})_3$
	95.4	95.51	4.55	4.49	—	—	ErOOH
	78.15	78.30	3.75	3.69	15.20	18.01	$\text{Er}(\text{OH})\text{CO}_3$
	67.1	67.28	9.60	9.50	23.2	23.22	$\text{Er}_2(\text{CO}_3)_3 \cdot 3\text{H}_2\text{O}$
	89.72	89.68	—	—	10.30	10.32	$\text{Er}_2\text{O}_2\text{CO}_3$
Ln = Tm	87.7	87.72	12.20	12.28	—	—	$\text{Tm}(\text{OH})_3$
	95.5	95.55	4.42	4.45	—	—	TmOOH
	78.5	78.45	3.63	3.66	17.85	17.89	$\text{Tm}(\text{OH})\text{CO}_3$
	67.41	67.47	9.48	9.44	23.15	23.09	$\text{Tm}_2(\text{CO}_3)_3 \cdot 3\text{H}_2\text{O}$
	77.1	77.09	2.41	2.40	20.50	20.51	$\text{Tm}_6(\text{OH})_4(\text{CO}_3)_7$
	86.0	86.16	4.0	4.02	10.0	9.82	$\text{Tm}_2\text{O}(\text{OH})_2\text{CO}_3$
	89.81	89.76	—	—	10.20	10.24	$\text{Tm}_2\text{O}_2\text{CO}_3$

Table 2. Unit cell parameters of more common phases.

Phase	$a(\text{Å})$	$b(\text{Å})$	$c(\text{Å})$	β	Crystal system
$\text{Er}(\text{OH})_3$	6.250	—	3.551	—	Hexagonal
ErOOH	5.935	3.622	4.505	109.3°	Monoclinic
$\text{Er}(\text{OH})(\text{CO}_3)$	4.963	8.452	7.201	—	Orthorhombic
$\text{Er}_2\text{O}_2\text{CO}_3$	3.821	—	14.984	—	Hexagonal
$\text{Er}_2(\text{CO}_3)_3 \cdot 3\text{H}_2\text{O}$	6.182	9.220	15.423	—	Orthorhombic
$\text{Tm}(\text{OH})_3$	6.230	—	3.501	—	Hexagonal
TmOOH	4.251	3.588	6.014	112.2°	Monoclinic
$\text{Tm}(\text{OH})\text{CO}_3$	4.960	8.449	7.198	—	Orthorhombic
$\text{Tm}_2\text{O}_2\text{CO}_3$	3.781	—	15.165	—	Hexagonal
$\text{Tm}_2(\text{CO}_3)_3 \cdot 3\text{H}_2\text{O}$	6.180	9.215	15.420	—	Orthorhombic

are also presented in table 3, though no indexing has been attempted. However, their identity as separate phases is substantiated by these data.

IR adsorption spectra of all the stable phases have been recorded. Only the spectra of $\text{Tm}_6(\text{OH})_4(\text{CO}_3)_7$, $\text{Tm}_2\text{O}(\text{OH})_2\text{CO}_3$ and those of the metastable phases are presented in figure 5. The number of absorption bands indicates that the CO_3^{2-} ions have the site symmetry of C_s or C_{2v} in all the cases; hence the notations of Gatehouse *et al* (1958) are followed in figure 5. CO_3^{2-} ion may be coordinated to the metal ion in more than one way, giving rise to unidentate or bidentate complexes. Fujita *et al* (1962) have shown that the extent of splitting ($\nu_3-\nu_1$) can be taken as an approximate index where the unidentate carbonate ($\sim 100\text{ cm}^{-1}$) has lower splitting than bidentate ion ($\sim 300\text{ cm}^{-1}$). Complication arises from the fact that there are more absorption bands than can be expected from the six theoretical fundamentals of CO_3^{2-} ion with C_s or C_{2v} symmetry. Caro *et al* (1972) have suggested that there may be more than one kind of site in the crystal structure for carbonate ions. This would multiply the corresponding

Table 3. X-ray powder diffraction data for the newer phases from $\text{Tm}_2\text{O}_3\text{-H}_2\text{O-CO}_2$ system.

$\text{Tm}_6(\text{OH})_4(\text{CO}_3)_7$			$\text{Tm}_2\text{O}(\text{OH})_2\text{CO}_3$			$\text{Tm}_6\text{O}_2(\text{OH})_8(\text{CO}_3)_3$		$\text{Tm}_4(\text{OH})_6(\text{CO}_3)_3$	
<i>d</i> (Å)	<i>I</i>	<i>hkl</i>	<i>d</i> (Å)	<i>I</i>	<i>hkl</i>	<i>d</i> (Å)	<i>I</i>	<i>d</i> (Å)	<i>I</i>
6.003	w	010	6.2115	vvs	100	12.10	29	9.92	20
4.701	vvs	002	4.288	ms	110	4.982	28	9.02	98
3.874	ms	110	3.200	s	014	4.268	29	6.071	100
4.694	vw	012	2.987	ms	020	4.009	43	5.212	37
3.913	mw	—	2.751	s	210	3.913	40	5.037	13
2.987	s	020	2.696	w	015	3.022	100	4.982	15
2.885	mw	—	2.571	w	204	2.618	43	4.772	10
2.526	ms	022	2.363	m	214	1.852	36	4.646	95
2.476	m	201	2.257	ms	124	1.583	21	4.538	6
2.349	s	004	2.150	ms	220			4.228	20
2.262	vw	122	1.951	s	224			4.101	17
2.102	mv	212	1.920	w	304			4.018	13
2.011	mw	—	1.585	w	133			3.930	20
1.941	m	220	1.764	vw	034			3.769	20
1.850	s	130	1.722	ms	108			3.722	22
1.830	ms	032	1.675	w	231			3.655	11
1.794	s	015	1.650	vw	231			3.583	10
1.706	m	300	1.616	w	028			3.415	11
1.678	m	301	1.599	w	128			3.336	6
1.562	vw	230						3.268	39
1.497	mw	040	$a = 6.195 \text{ \AA}$					3.213	9
1.428	mw	206	$b = 5.974 \text{ \AA}$					3.108	54
1.276	m	400	$c = 15.158$					3.037	9
1.249	vw	332	$\beta = 97.5^\circ$					3.018	10
$a = 5.118 \text{ \AA}$			Monoclinic					2.968	9
$b = 5.989 \text{ \AA}$								2.871	11
$c = 9.398 \text{ \AA}$								2.839	10
Orthorhombic								and 16 other lines	

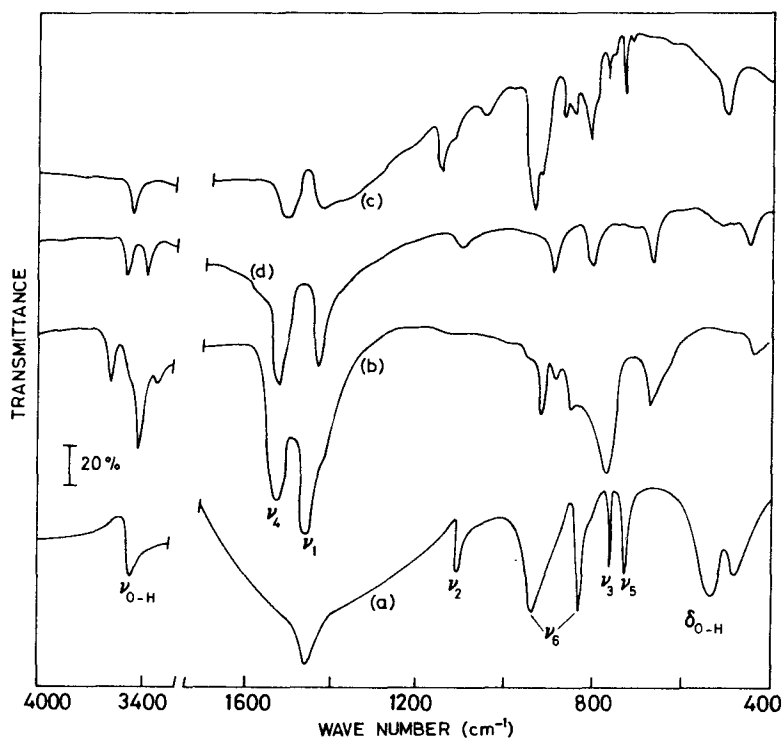


Figure 5. IR spectra of a. $\text{Tm}_6(\text{OH})_4(\text{CO}_3)$, b. $\text{Tm}_2\text{O}(\text{OH})_2\text{CO}_3$, c. $\text{Tm}_4(\text{OH})_6(\text{CO}_3)_3$ and d. $\text{Tm}_6\text{O}_2(\text{OH})_8(\text{CO}_3)_3$.

number of fundamentals. A combination of fundamental vibrational modes with lattice modes may give additional bands. Splitting of nondegenerate out-of-plane deformation (ν_6) is a definite evidence for the non-equivalent orientation of CO_3^{2-} ion. The stretching (around 3600cm^{-1}) and librational modes (around 550cm^{-1}) for the $(\text{OH})^{-1}$ groups can be noticed in figure 5.

4. Conclusions

There is increased complexity in $\text{Ln}_2\text{O}_3\text{-H}_2\text{O-CO}_2$ phase diagrams of the heavier lanthanides. Additional phases stabilised in Tm_2O_3 system are $\text{Tm}_2\text{O}(\text{OH})_2\text{CO}_3$ and $\text{Tm}_6(\text{OH})_4(\text{CO}_3)_7$. Other stable phases common to Er and Tm are $\text{Ln}(\text{OH})_3$, $\text{Ln}_2(\text{CO}_3)_3 \cdot 3\text{H}_2\text{O}$, LnOOH , $\text{Ln}(\text{OH})\text{CO}_3$ (orthorhombic) and Ln_2O_3 . In the presence of minor impurities like alkali ions, $\text{Tm}_6\text{O}_2(\text{OH})_8\text{CO}_3$ and $\text{Tm}_4(\text{OH})_6(\text{CO}_3)_3$ are metastably formed. The general hydrothermal behaviour of $\text{Ln}_2\text{O}_3\text{-H}_2\text{O-CO}_2$ system indicates marked differences in the chemical equilibria of heavier lanthanides when compared to those prevailing in lighter lanthanides.

References

- Caro P, Sawyer J and Eyring L 1972 *Spectrochim. Acta* **A28** 1167
 Caro P and Lemaitre-Blaise M 1970 *Compt. Rend. (Paris)* **C269** 677

- Chai B H T and Mroczkowski S 1978 *J. Cryst. Growth* **44** 93
- Christensen A N 1970 in *Les Elements des Terres Rares Colloq. Intern. Du CNRS* No. 180, Vol. 1, (CNRS, Paris) p. 279
- Christensen A N 1973 *Acta Chem. Scand.* **27** 1835, 2973
- Dexpert H, Lemaitre-Blaise M and Caro P 1972 in *Reactivity of solids* (ed) J Mitchell (London: Chapman and Hall) 758
- Fujita J, Martell A E, Nakamoto K and Kobayashi M 1962 *J. Chem. Phys.* **36** 339
- Gatehouse B M, Livingston S E and Nyholm R S 1958 *J. Chem. Soc.* 3137
- Kutty T R N, Viswanathiah M N and Tareen J A K 1978 *Proc. Indian Acad. Sci. (Chem. Sci.)* **87** 69
- Sawyer J, Caro P and Eyring L 1973 *Rev. Chim. Miner.* **10** 93
- Tareen J A K and Kutty T R N 1980 *J. Cryst. Growth* **50** 527
- Tareen J A K, Kutty T R N and Krishnamurthy K V 1980a *J. Cryst. Growth* **49** 761
- Tareen J A K, Kutty T R N and Mohamed I 1980b *Indian Mineral* **21** 43
- Viswanathiah M N, Kutty T R N, Rao N B and Tareen J A K 1978 *J. Cryst. Growth* **44** 366'